POPULAR SUMMARY

Sensitivity of Middle Atmospheric Analysis to the Representation of Gravity Wave Drag
(To be submitted to Journal of Geophysical research – Atmospheres)

Shuhua Li, Steven Pawson, Byron A. Boville, Shian-Jiann Lin

Understanding the structure of the middle atmosphere is important for studies of atmospheric chemistry and the terrestrial radiation balance. Data assimilation provides a means of estimating the full time-dependent, three-dimensional structure of winds, temperature, and heights from observations of a limited number of these variables at reduced spatial and temporal resolution. For the middle atmosphere, the only operational data source is near-nadir radiance measurements from Tiros Operational Vertical Sounders, which can be used to infer the thermal structure. The data assimilation process involves combining these data with short forecasts from a General Circulation Model (GCM),
which includes representations of all known physical processes in the atmosphere. This study examines sensitivity to the sub-grid-scale gravity-wave drag (GWD), which is poorly constrained by observations, yet must be represented in GCMs in order for simulations of climate to be credible. A suite of assimilation experiments, including seasonal and medium-range forecasts, was conducted for August 1999, in which the GWD was varied. The main impacts of the representation of GWD on analyzed temperature are shown to be near the stratopause in winter (in the Antarctic), where the impacts of including or neglecting a spectrum of gravity waves was shown to have an impact of almost 10K on the analyzed temperature. In this region, the medium-range forecasts show a rapid model drift (to lower temperatures) when these waves are neglected. These experiments demonstrate the impact of a model bias on the resultant analyses. A major reason for this is that the TOVS data themselves are only a weak constraint: the deep weighting functions mean that the radiances can constrain only thick atmospheric layers. It is demonstrated that the best consistency between the GCM and the TOVS data is when the most complete spectrum of waves is used for the GWD, and that neglecting these waves results in deficient analyses.

Sensitivity of Middle Atmospheric Analysis to the Representation of Gravity Wave Drag

Shuhua Li, Steven Pawson

Goddard Earth Sciences and Technology Center, University of Maryland Baltimore County, and Global Modeling and Assimilation Office, NASA Goddard Space Flight Center

Byron A. Boville

National Center for Atmospheric Research

S.-J. Lin

NOAA Geophysical Fluid Dynamics Laboratory

Key words: sensitivity, assimilation, middle atmosphere, gravity wave drag.

Short title: SENSITIVITY OF ANALYSIS TO GRAVITY WAVE DRAG

Abstract. This study examines the sensitivity of middle atmospheric analyses to the representation of gravity wave drag (GWD) in the general circulation model (GCM). A strong sensitivity of temperatures near the stratopause to the inclusion and representation of waves with non-zero phase speeds is isolated; this is consistent with the induced mean meridional circulation. The change (between a control analysis and one with no GWD) decreases with decreasing altitude and has a vertical structure with alternating positive and negative differences that are caused by the constraint on thick-layer radiances offered by near-nadir sounding radiometers. Without the non-zero phase-speed GWD, there is a large "observation minus forecast" residual that is substantially smaller when these waves are included, indicating the need for these waves in the GCM. Moreover, the sensitivity of analyzed temperatures to the inclusion of these waves reveals the importance of using a non-biased GCM in regions where the observational constraint (thick-layer radiances) is indirect.

1. Introduction

Chemical processes in the middle atmosphere play an important role in the climate system, largely because of their impacts on ozone, one of the most important radiatively active gases in the atmosphere. Because of this, there is a need for knowledge of the state of the thermal structure, transport characteristics and composition of the stratosphere and mesosphere. Various analysis techniques have been developed to estimate the meteorological state of the middle atmosphere. Randel et al. [2004] show some considerable uncertainty among estimates of the temperature near the stratopause. Relatively few ground-based measurements of temperature above the middle stratosphere are presently available, which means that it must be derived directly (by inversion) or indirectly (by assimilation techniques) from space-based radiance measurements. The present study focuses on uncertainties in the analyzed middle atmospheric structure in a data assimilation system (DAS) that result from a combination of uncertainties in inverting nadir radiance measurements and the treatment of gravity-wave drag in a numerical model.

Atmospheric data assimilation is a potentially powerful technique for producing analyses of meteorological fields and constituents. It utilizes optimal estimation techniques to combine observations with forecasts produced using deterministic models (see Cohn 2001, for example) to yield time-dependent, three-dimensional analyses. While numerous other techniques can be (and are) applied to meteorological data, a powerful attribute of data assimilation is the formal mathematical development of the

methodology, which facilitates examination of errors in the system and also allows for effective combination of multiple types of observations. The Goddard Earth Observation System, Version 4 (GEOS-4) DAS used in this study combines in-situ temperatures and winds (mainly from radiosondes) with space-based estimates of the thermal structure and numerous other data types, which are important in the troposphere. The main data type for the upper stratosphere is nadir-sounding radiance measurements: the present study utilizes level-1b radiances from the Tiros Operational Vertical Sounder (TOVS) instruments, which has a limited vertical resolution because of the physical nature of nadir emission.

An important component of the DAS is the deterministic model, which for meteorological applications is a general circulation model (GCM). Climate model studies have revealed that the middle atmosphere is extremely sensitive to the representation of sub- grid-scale gravity wave drag (GWD), which is parameterized in GCMs. While "mountain waves" must be included in tropospheric models [e.g., Palmer et al., 1985], it is also important to include waves with non-zero phase speeds in the middle atmosphere [e.g., Rind et al., 1988; Garcia and Boville, 1994]. Such waves are forced by processes such as convection or shear instabilities. Important as these waves are for climate studies, there has been little investigation of their impact on the assimilated meteorology of the middle atmosphere. Omitting such waves from the GCM can be expected to lead to a bias in the forecast, and it is important to understand how the available observations are able to correct for such biases.

By way of introduction, Fig. 1 shows the zonal-mean temperature at 1hPa

from several datasets for July 1992. The GEOS-4 analyzed temperature is about 10K lower than the warmest dataset, from the National Centres for Environmental Prediction (NCEP) Climate Prediction Centre (CPC). The NCEP CPC temperatures are determined by direct inversion of the TOVS radiances using climatological temperature profiles as a first guess, while GEOS-4 ingests the radiances and uses the GCM forecasts as a first guess [Joiner and Rokke, 2000]. Analyses from the United Kingdom Meteorological Office (UKMO), which use retrieved temperatures in a DAS [Swinbank and O'Neill, 1995], lie between the two extremes, but are slightly closer to the GEOS-4 values. Two additional datasets are shown; these are both derived from limb-sounding instruments on the Upper Atmosphere Research Satellite (UARS); Microwave Limb Sounder (MLS) estimates are somewhat colder than the NCEP CPC data at all latitudes, while Halogen Occultation Experiment (HALOE) data show more variations with latitude, with extreme scatter in the southern middle latitudes. Both the MLS and HALOE estimates, being from limb-sounding instruments, have higher vertical information content than the nadir- sounding TOVS data, so could resolve a sharper stratopause. As a microwave emission measurement, MLS data can be inverted to estimate temperatures at a wide range of latitudes for each day. Wu et al. [2003]document a slight warm bias in the stratosphere and a cold bias in the mesosphere. HALOE scans through the range of latitudes as the month progresses, so the North-South structure is undersampled: this may explain the noisiness in the latitudinal structure and the large deviation from other estimates in the winter hemisphere. Remsberg et al. [2002] note the very small bias in HALOE temperatures

between the middle stratosphere and lower mesosphere.

This work examines the sensitivity of the analyses using TOVS data to the underlying GCM. The two most relevant curves in Fig. 1 are thus for GEOS-4 the UKMO, whose differences must be attributed to the retrieval mechanisms and the models. The present study examines uncertainty within the framework of the GEOS-4 assimilation system. An outline description of the GEOS-4 DAS is given in section 2. The results are presented in section 3. The final section discusses the results in the context of our understanding of the atmosphere.

2. Description of the GEOS-4 DAS

The GEOS-4 DAS is build around the so-called finite-volume (fv) GCM and the Physical-space Statistical Analysis Scheme (PSAS). Relevant aspects of each of these are summarized here, followed by slightly more detailed descriptions of the representation of sub-grid-scale gravity-wave drag and the TOVS data.

2.1 Overview of the System

The fvGCM is based on the flux-form, semi-Lagrangian formulation of the Navier-Stokes Equations, with a floating vertical coordinate [Lin and Rood, 1997; Lin, 1997; Lin, 2004]. This is a state-of-the-art dynamical core, which has been demonstrated to have excellent conservation properties for vorticity, momentum and mass, as well as an ability to maintain tracer-tracer correlations [Lin and Rood, 1997]. Physical parameterizations are based on those described by Kiehl et al. [1998], developed for the

Community Climate Model, Version 3 (CCM3) at the National Center for Atmospheric Research. The model domain extends from the surface to 0.01hPa (near 80 km), with 55 layers and a vertical resolution slightly more than 1 km in the lower stratosphere.

Observations are combined with the model forecasts using a sequential technique with a timestep of six hours. Data from three hours each side of the synoptic times (0000, 0600, 1200, 1800) are accumulated for each analysis step. The statistical analysis technique used is PSAS [Cohn et al., 1998], which works in observation space (model forecasts are interpolated to observation locations), rather than the more conventional techniques that use model space. This should have little impact on the present results. In the present study, the analyses were performed on a subset of the model levels, using every second level in the middle atmosphere. There is no constraint from observations above the lower mesosphere.

All experiments performed for this study were made at a horizontal resolution of 2.5 longitude by 2 latitude. This choice of resolution is half that normally used in GEOS-4, but this should not impact the results in any substantial manner.

2.2 Sub-Grid-Scale Gravity Wave Drag

The standard version of CCM3 included a GWD scheme for mountain waves, after [McFarlane, 1987], with a momentum-deposition scheme based on a saturation condition, following Lindzen [1981]. These mountain waves are excited by the distribution of sub-grid-scale orographic variance on the model grid, with strength and direction proportional to the vector wind at the source level, assumed to be twice the standard

deviation of the topographic variance.

Garcia and Boville [1994] extended the mountain-wave scheme to waves with non-zero phase speeds and, in agreement with Rind et al. [1988] and other work, Boville [1995] demonstrated the importance of such waves for forcing a realistic climate state in the mesosphere and stratosphere. This "nine-wave" model, with a mountain wave and four waves traveling in each direction, is used in this study. The four waves are assigned phase speeds of 10, 20, 30 and 40 ms^{-1}. They are launched at 100hPa with amplitudes of 6.4 km and horizontal wavelengths of 100 km. Note that such waves would not be resolved in a GCM until the horizontal resolution decreased to about 25 km, or about 0.25 in middle latitudes. No spatial structure is assigned to the source of these waves with non-zero phase speeds, since there is little observational constraint on this, and recent work [e.g., Alexander et al., 2000] is inconclusive about the details of any coupling between (say) convective towers and the gravity-wave spectrum in the atmospheric column above the cloud.

Additionally, a small background gravity-wave stress (assumed to be from waves with zero phase speed) is applied to all gridpoints of the model. This leads to a weak drag in the mesosphere over the oceans, which serves to close the stratospheric jets.

2.3 Middle Atmospheric Data

The in-situ observational network for the upper atmosphere, comprising of sondes, aircraft winds, etc., becomes less dense with increasing altitude. In the middle stratosphere there are virtually no direct measurements, so there is an increased reliance

on space-based radiance observations to constrain the analyses. There are two major implications from this. First, no wind data are available to constrain the system, so the analyses are strongly dependent on the balance assumed between thermal structure and winds (in this case, geostrophic balance is imposed). Second, the operational sensors used in this study measure infrared emission at (and about) the nadir view, resulting in a limited vertical resolution. The studies performed here were for August 1998, when NOAA-16 TOVS data were available. The main instrument for the middle and upper stratosphere was the Stratospheric Sounding Unit (SSU), which contains essentially three pieces of information for an atmospheric layer that is about 20 km thick [e.g., Bailey et al., 1993].

3. Results

3.1 Impacts of non-zero phase speed waves on meteorological analyses

A number of experiments have been conducted to examine the impacts of the GWD on the assimilations. The two extreme configurations are the control run, with all nine gravity waves, and the no-GWD run. The initial discussion focuses on differences in the analyses produced using these two model configurations. Monthly mean analyzed 1-hPa temperature for August 1998 reveal that the largest differences between these two assimilations are in the high-latitude southern hemisphere. Note that this level is close to the stratopause and near the highest level where the TOVS data contain information. In the northern (summer) hemisphere, differences are less than 1K. In the Tropics,

there is a slight cooling when the GWD is omitted. In the southern middle latitudes, there is little impact in the region where the dominant planetary wave structure shows up in the analysis. In the Antarctic there is a very large impact, with temperature differences approaching 30K. The dominant signal in these differences is zonal, which allows consideration of the zonal-mean state in the future discussion.

Latitude-height sections of zonal-mean wind and temperature (Fig. 3) for the same two cases confirm that the predominant differences between the nine-wave and no-wave cases are in the upper stratosphere and mesosphere at high southern (winter) latitudes. Recall that the physical process under investigation, the GWD, acts primarily on the momentum forcing, while the data constraint is on the temperature. The differences in zonal-mean zonal wind are largest in the mesosphere, with peaks near the latitude of the jet maximum and in the Tropics. These changes are broadly consistent with the GWD distributions in the two analyses, where there is only a weak westerly wind forcing (from the background spectrum) above about 55 km in the mountain-wave drag, but large drag from the non-zero phase-speed waves (Fig. 4).

Changes in temperature are largely in thermal wind balance with the wind differences (Fig. 3), a consequence of the induced mean meridional circulation at the highest levels. For free-running models, the dipolar temperature differences between the nine-wave and no-wave simulations extend from the mesosphere until well down into the stratosphere because of the structure of the induced meridional circulation ("downward control") induced by the GWD. Differences in these analyses (Fig. 4) deviate from this structure because of the data constraint. The measurement of radiance places a

constraint on the total outgoing energy, meaning that warming the atmosphere at any level because of a dynamical constraint in the model will necessitate a cooling at other levels (in this case below). The negative temperature difference, of about 10K, near 40 km at the South Pole is a consequence of this compensation in the analyses. A similar effect, with opposite sign because of the dipolar structure that arises from dynamical forcing, is evident near 50°S. Below 35 km, differences are very small: this is largely because of the GWD having the strongest impact at high levels, but also because there are more conventional data (especially wind measurements) below the middle stratosphere.

Fig. 4 clearly shows that the mountain wave drag has an impact only in the stratosphere, with a double maximum that acts on each flank of the polar night jet; there is only a small mountain-wave drag in the mesosphere, where (in the nine-wave experiment) the drag reaches very large values. While the predominant focus of this study is on the Antarctic region, it is noted here that there is substantial wave drag in the tropics and in the northern (summer) hemisphere that leads to discernable localized differences in the wind in the mesosphere. In the tropical mesosphere, the wind changes sign (from westerly to easterly) when only mountain waves are included in the model, but the small direct component of the thermal impact of the gravity waves leads to a small response in temperature at these upper levels; at the stratopause and below, where the data constrain the system, there is little impact away from the Antarctic.

3.2 Sensitivity experiments: analyses and forecasts

A series of experiments has been conducted to examine some of the mechanisms at work and the sensitivities of the results to more details of the GWD. These experiments include the two extreme model configurations discussed above (nine-wave and mountain-wave runs), as well as systems with five waves or no waves at all. The control (nine-wave) run includes gravity waves with phase speeds of 0, ± 10, ± 20, ± 30, ± 40 ms^{-1}. The five-wave system excludes the four waves with the largest phase speeds, while the no-wave run excludes even the mountain waves.

The first set of experiments compare seasonal forecasts made with each of the four model configurations with the corresponding analyses. The experiments were initialized on July 21, 1999 and run through August. Time series of area-mean temperature in the polar cap at 1hPa show divergence between the different configurations (Fig. 5). The main results are listed here:

(a) The five-wave analysis differs by around 3-5K from the nine-wave analysis throughout the duration of the experiment. This is consistent with a weaker adiabatic descent in the five-wave case, since there is less forcing in the mesosphere.

(b) The analyses with or without any non-zero phase speed gravity waves differ substantially from each other. For most of August, the difference between the nine-wave and the no-wave cases exceeds 10K. There is almost no difference in polar-averaged temperature in the no-wave and mountain-wave cases, because the drag from the mountain wave almost vanishes in the mesosphere (Fig. 4).

(c) The seasonal forecasts produced by model configurations depend strongly on the inclusion of non-zero phase speed gravity waves. As expected from climate model studies (e.g., Rind et al., 1988), omitting these waves leads to substantial biases in the model simulations, with temperatures of 210-215K in August, compared to 250-260K in the five-wave or nine-wave configurations. These latter forecasts closely follow the corresponding analyses. (Note that these are only single cases, initialized on the same day as the analyses, so perfect agreement is not expected.) There is a large discrepancy between forecast and analysis when the non-zero phase speed waves are omitted from the model, indicating that insertion of data can lead to substantial corrections of a biased model, but (coupled with point (a) above) the correction is not complete.

A series of ten-day forecasts have been made using the control (nine-wave) analysis as initial fields and each of the four model configurations. Seven forecasts were made, initialized on July 21, July 26, August 1, 6, 11, 16, and 21. The results for the first five days (Fig. 6) show the rapid cooling of the polar stratopause region when the non-zero phase speed waves are omitted, but that the forecasts generally trace the analyses reasonably well when these waves are included. This is shown more quantitatively in Fig. 7, where the "analysis minus forecast" (A-F) for the nine-wave run is shown as a function of forecast day for each of the seven ten-day forecasts. At 1hPa there is a tendency for the forecast to be too cool, with clustering at negative values of A-F, but with some positive values. At 10hPa the opposite occurs, with a tendency to warm with time from the analyses. This indicates that even the best model version in this study has a tendency to bias the medium-range forecast.

Additional information about the performance of the analysis system is given by the "observation minus forecast" (O-F) tendency of geopotential height at 1hPa (Fig. 8). This quantity describes the agreement between the observations used in the assimilation system and the background (six-hour) forecast. The O-F shows little difference away from the highest southern latitudes, where there is a strong relationship between the number of gravity waves in the model and the agreement between model and forecast. The smallest O-Fs, less than 15gpm, are for the nine-wave model, while the largest values (reaching about 55gpm) are for the no-wave model. This result shows that degrading the model (by omitting a large part of the gravity-wave spectrum) leads to a larger disagreement between forecast and data, as well as in a degradation of the analysis.

The largest affects of the GWD are on the analyses at high latitudes, where there are no independent validation data. HALOE data are available in the southern middle latitudes in August 1998, and a composite profile near 56°S for Aug. 24-28 is used for validation. The comparison reveals a superior quality of the mean assimilated temperature profile at this latitude, with a higher temperature that is closer to HALOE values in the 48-52 km range. This corrects what is a cold bias throughout the middle and upper stratosphere, but has no impact on the analyses below about 35 km and slightly increases the cold bias between about 35 and 45 km (because of the radiance balancing). This could be because of an inherent bias between the HALOE and TOVS instruments, investigation of which is well beyond the scope of this study.

4. Conclusions and Discussion

A number of assimilation experiments have been performed to examine the sensitivity of stratospheric meteorological analyses to the formulation of the prediction model. The experiments focused on the impacts of inclusion of non-orographic GWD in the GCM, this being the major uncertain factor in the modeling of the upper stratosphere and mesosphere. The experiments used a relatively simple formulation of GWD, with a discrete, coarse-resolution spectrum of waves imposed in the lower stratosphere, employing a momentum deposition scheme based on Lindzen (1982). The experiments, performed for August of 1998, reveal a strong sensitivity in the analyzed temperatures in the winter polar stratosphere.

The most detailed GWD module, with one mountain wave and eight traveling waves, yielded the "best" analyses when compared to the few independent measures of temperature available at these levels (HALOE data, Fig. 9). Omitting all waves with non-zero phase speeds resulted in a substantially (8-10K) lower temperature at 1hPa in the analyses, while omitting only the waves with the fastest phase speeds had a small impact (about 2K cooling). Tunable parameters for the GWD code were adapted to give a "good" climate simulation with a free-running version of the GCM, so the superior performance of this configuration does not warrant further discussion. The most important point is that as waves are omitted from the GWD "spectrum" there is a detrimental impact on the analyses in the upper stratosphere. Near the stratopause, this impact is consistent with the reduction in momentum forcing in the mesosphere:

less forcing leads to a stronger jet and a weaker induced mean meridional circulation, so that the polar region is colder (consistent with thermal wind balance). While this result is well known for free-running GCMs (e.g., Rind et al., 1988), it is not immediately obvious that it would carry over into assimilated datasets.

Direct observations of temperature and wind in the upper stratosphere could be used as a strong data constraint on the assimilation system. However, routine observations of the upper atmosphere are based only on the near-nadir radiances (infrared emission) by the TOVS (and similar) space instruments. The physical nature of such measurements means that vertical resolution is low (only three pieces of information in the height range spanning about 30 to 55 km), so that the data constraint is quite weak. Use of such observations allows compensating biases to exist in the resulting analyses. A very simple argument is that if the temperature in the upper part of one channel is too low, then a warm bias is needed in the height range of the lower part of that channel; this translates to a warm bias in the upper part of the next lower channel, thus communicating the initial bias downwards in the atmosphere. This effect is clearly seen over Antarctica in the zonal-mean temperature difference between runs with and without the non-zero phase speed GWD (Fig. 3). This vertical structure in differences is very different to that in free-running GCMs when these waves are omitted, because there the impact of the changed mean meridional circulation is felt down to lower levels.

The impacts on the analyses result primarily from the poor vertical resolution of the TOVS radiance data. There is also a feedback in the assimilation system. In the implementation of the Joiner and Rokke (2000) scheme, radiances are inverted to yield

temperature, using the first-guess (six-hour forecast) as the a priori. This means that the "observed" state depends on the "forecast" state, in a manner determined by the weights given to the a priori in the retrieval. This feedback, in the presence of a biased model, essentially leads to contamination of the retrievals so that the full impact of the data is not necessarily realized. However, because of the low vertical resolution of the TOVS data, it is highly likely that direct assimilation or radiances would yield the same effects, because the forecast bias cannot be corrected. In the present system, the TOVS data are able to correct somewhat for severe forecast bias (much larger O-Fs in the degraded GCM: Fig. 8) but are unable to fully correct the model bias (Fig. 5), which develops very rapidly in the free-running model (Fig. 6).

Uncertainties in the analyzed temperature arising from degrading the GWD in the GCM lead to temperature differences approaching 10K near the winter Antarctic stratopause. These are substantially smaller than those in the free-running model. This uncertainty is of similar size to the differences between datasets shown in Fig. 1, although the latitudinal structures suggest that the causes of those discrepancies are different.

The major conclusion of this work is that the analyzed temperature in the upper stratosphere depends very strongly on the formulation of the GCM. This results applies to systems that assimilate TOVS radiances, which arise from deep atmospheric layers. It points the way to the need for more information on the vertical thermal structure, as might be obtained from limb emission measurements. While these are available from research satellites, there is no time series of such data for "operational" data assimilation

or long-term reanalyses. There are also no dependable constraints on the winds, which would be very valuable for the analysis problem (especially in the tropics). Present research is directed at including limb-sounding estimates of the thermal structure and on the implementation of more realistic gravity wave drag schemes, for which the performance when confronted with data will be an important benchmark, alongside the performance of the free-running model.

Acknowledgements

This work was supported by NASA's Pathfinder Datasets and Associated Science Program, Grant NAG5-12162. We are grateful to numerous colleagues for fruitful discussions and technical assistance, especially Jiun-Dar Chern.

References

Alexander, M. J., and T. J. Dunkerton, A spectral parameterization of mean-flow forcing due to breaking gravity waves, *J. Atmos. Sci., 56*, 4167-4182, 1999.

Alexander, M. J., J. H. Beres, and L. Pfister, Tropical stratospheric gravity wave activity and relationships to clouds, *Geophys. Res. Lett., 105*, 22,299-22,309, 2000.

Bailey, M. J., A. O'Neill and V. D. Pope, Stratospheric analyses produced by the United Kingdom Meteorological Office, *J. Appl. Meteorol., 32*, 1472-1483, 1993.

Boville, B. A., Middle Atmosphere Version of CCM2 (MACCM2) - Annual cycle and interannual variability, *J. Geophys. Res. 100*, 9017-9039, 1995.

Cohn, S. E., A. da Silva, J. Guo, M. Sienkiewicz, and D. Lamich, Assessing the effects of data selection with the DAO physical-space statistical analysis system, *Mon. Wea. Rev., 126*, 2913-2926, 1998.

Coy, L., and R. Swinbank, Characteristics of stratospheric winds and temperatures produced by data assimilation, *J. Geophys. Res., 102*, 25,763-25,781, 1997.

da Silva, A., and S. J. Lin, The DAO physical-space/finite-volume data assimilation system, Part I: Algorithm theoretical basis for the "violet" core system, DAO Office Note 2000-NN, 27 pp.

Garcia, R. R., and B. A. Boville, Downward control of the mean meridional circulation and temperature distribution of the polar winter stratosphere, *J. Atmos. Sci., 51*, 2238-2245,1994.

Holton, J. R., The role of gravity wave induced drag and diffusion in the momentum budget of the mesosphere, *J. Atmos. Sci., 39*, 791-799, 1982.

Joiner, J., and L. Rokke, Variational cloud clearing with TOVS data, *Q. J. R. Meteorol. Soc., 126*, 725-748, 2000.

Kiehl, J. T., J. J. Hack, G. B. Bonan, B. A. Boville, D. L. Williamson, and P. J. Rasch, The National Center for Atmospheric Research Community Climate Model: CCM3, *J. Clim., 11*, 1131-1150, 1998.

Lin, S. J., and R. B. Rood, Multidimensional flux-form semi-Lagrangian transport schemes, *Mon. Wea. Rev., 124*, 2046-2070, 1996.

Lin, S. J., and R. B. Rood, An explicit flux-form semi-Lagrangian shallow water model on the sphere, *Q. J. Roy. Met. Soc., 123*, 2531-2533, 1997.

Lin, S. J., A "vertically Lagrangian" finite-volume dynamical core for global models, *Mon. Wea. Rev.*, in press, 2004.

Lindzen, R. S., Turbulence and stress owing to gravity wave and tidal breakdown, *J. Geophys. Res., 86*, 9707-9714, 1981.

Manney, G. L., J. L. Sabutis, S. Pawson, M. L. Santee, B. Naujokat, R. Swinbank, M. E. Gelman, and W. Ebisuzaki, Lower stratospheric temperature differences between meteorological analyses in two cold Arctic winters and their impact on polar processing studies, *J. Geophys. Res., 108*(D5), 8328, doi: 10.1029/2001JD001149, 2002.

McFarlane, N. A., The effect of orographically excited gravity wave drag on the general circulation of the lower stratosphere and troposphere, *J. Atmos. Sci., 44*, 1775-1800, 1987.

Palmer, T. N., G. J. Shutts and R. Swinbank, Alleviation of a systematic westerly bias in general circulation and numerical weather prediction models through an orographic gravity wave drag parametrisation. *Q. J. R. Meteorol. Soc., 112*, 1001–1039, 1986.

Randel, W. J., P. Udelhofen, E. Fleming, M. Geller, M. Gelman, K. Hamilton, D. Karoly, D. Ortland, S. Pawson, R. Swinbank, F. Wu, M. Baldwin, M.-L. Chanin, P. Keckhut, K. Labitzke, E. Remsberg, A. Simmons and D. Wu., The SPARC intercomparison of middle atmosphere climatologies, *J. Clim.*, in press, 2004.

Remsberg, E. E., L. Deaver, J. Wells, G. Lingenfelser, P. Bhatt, L. Gordley, R. Thompson, M. McHugh, J. M. Russell, P. Keckhut, and F. Schmidlin, An assessment of the quality of Halogen Occultation Experiment temperature profiles in the mesosphere based on comparisons with Rayleigh backscatter lidar and inflatable falling sphere measurements, *J. Geophys. Res., 107*(D20), 4447, doi: 10.1029/2001jd001521, 2002.

Rind, D., R. Suozzo, N. K. Balachandran, A. Lacis and G. Russell, The GISS Global

Climate-Middle atmosphere model. Part 1: Model structure and climatology. *J. Atmos. Sci., 45*, 329–370, 1988.

Schubert, S. D., R. B. Rood, and J. Pfaendtner, An assimilation dataset for Earth science applications, *Bull Am. Meteorol. Soc., 74*, 2331-2342, 1993.

Wu, D. L., W. G. Read, Z. Shippony, T. Leblanc, T. J. Duck, D. A. Ortland, R. J. Sica, P. S. Argall, J. Oberheide, A. Hauchecorne, P. Keckhut P, C. Y. She, and D. A. Krueger, Mesospheric temperature from UARS MLS: retrieval and validation, *J. Atmos. Sol. Terr. Phys., 65*, 245-267, 2003.

B. Boville, NCAR, P.O. Box 3000, Boulder, CO 80307.

S. Li, Code 900.8, NASA Goddard Space Flight Center, Greenbelt, MD 20771.

(sli@gmao.gsfc.nasa.gov)

S.-J. Lin, NOAA Geophysical Fluid Dynamics Laboratory, Princeton, NJ 08544

S. Pawson, Code 900.3, NASA Goddard Space Flight Center, Greenbelt, MD 20771.

Received _____

Figure captions

Figure 1. Monthly mean temperature at 1 hPa in July 1992 from two independent observations (HALOE and MLS), the NCEP-CPC prediction, and assimilations from GEOS-4 and UKMO. The latitudinal resolution for HALOE and MLS is 1°, while the resolution for GEOS-4 and UKMO is 2° and 2.5° respectively. The resolution of NCEP-CPC is abut 4.44° in latitude.

Figure 2. Analyzed global temperature at 1 hPa averaged for August 1999: (a) control, and (b) no-GWD (gravity wave forcing removed). The contour interval is 2.5 K.

Figure 3. Latitude-altitude cross section of analyzed temperature and zonal wind from the control analysis and no-GWD analysis averaged for August 1999. The bottom two show the differences between the two situations, and regions with positive difference are shaded.

Figure 4. Tendency of zonal wind due to gravity wave drag averaged for August 1999. The units are m/s per day.

Figure 5. Time series of zonal mean temperature at 1 hPa from analysis and forecast only during July-August 1999, averaged over 60-90°S.

Figure 6. Time series of zonal mean temperature at 1 hPa from 5-day forecast using the control analysis as the reference state. The temperature is averaged over 60-90°S.

Figure 7. Scatter plots of globally-averaged temperature bias (analysis minus forecast) for 10-day forecast versus forecast length: (a) 1 hPa; (b) 10 hPa. The individual forecast runs use control analysis as the reference state.

Figure 8. Zonal mean O-F (observation minus forecast) residuals of geopotential height at 1 hPa averaged for August 1999.

Figure 9. Temperature profile at 56°S averaged for 24-28 August, 1999. The temperature profiles are plotted for HALOE and GEOS-4 with/without GWD forcing.

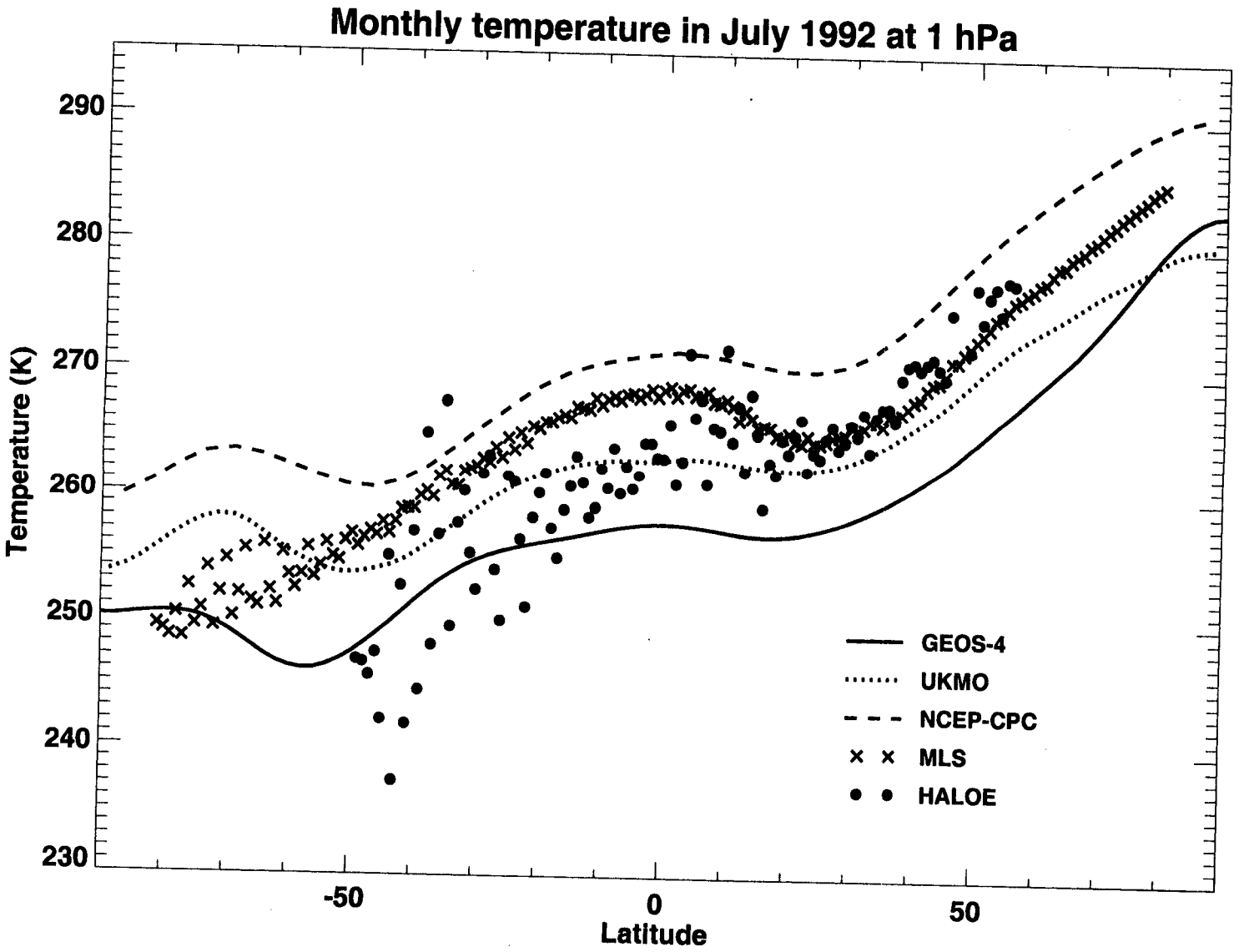
Monthly temperature in July 1992 at 1 hPa
Temperature (K)
290
280
270
260
250
240
230
-50
0
50
Latitude
GEOS-4
UKMO
NCEP-CPC
MLS
HALOE

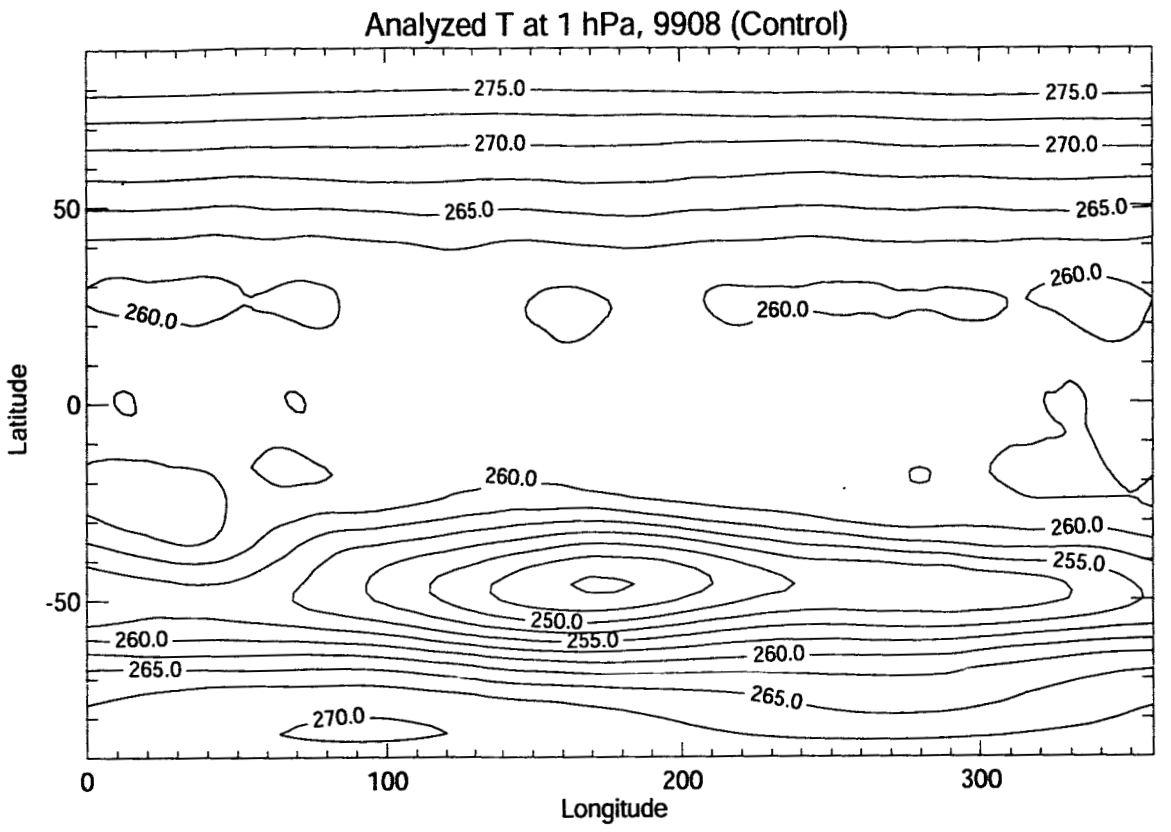
Analyzed T at 1 hPa, 9908 (Control)
275.0
270.0
265.0
260.0
255.0
250.0
50
0
-50
Latitude
0
100
200
300
Longitude

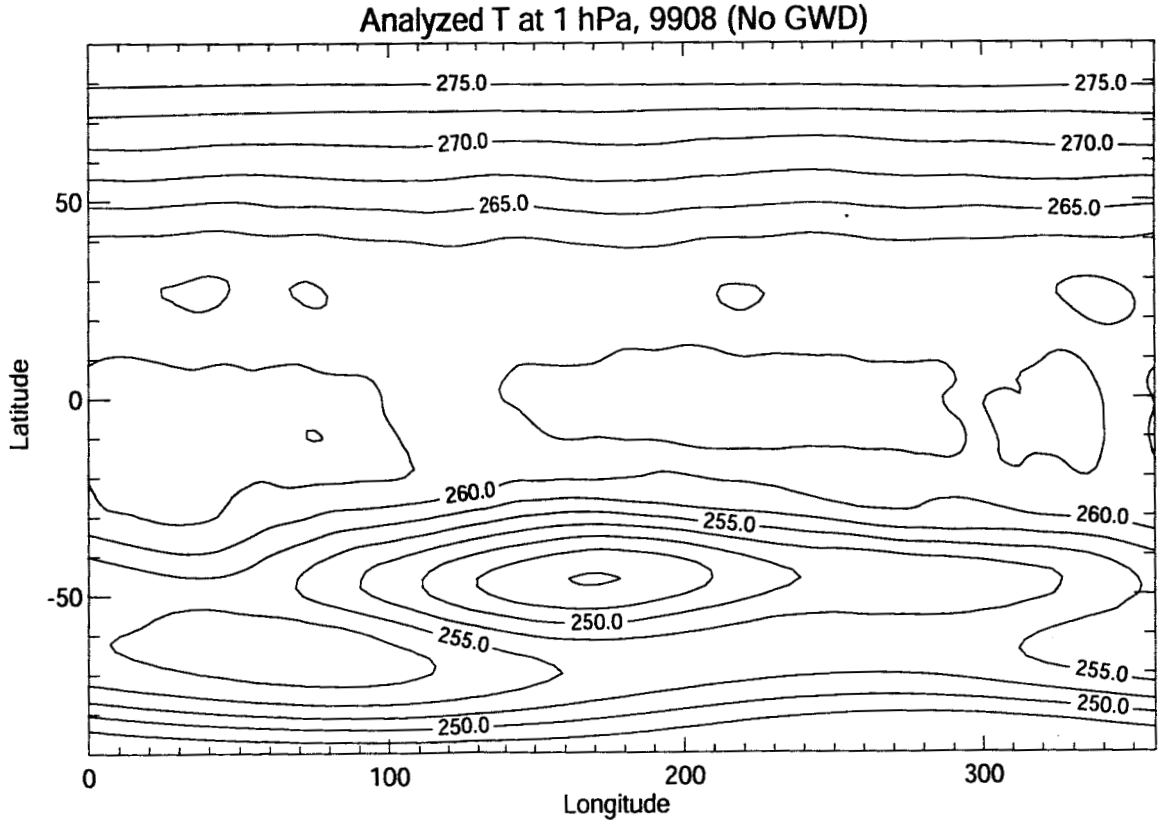
Analyzed T at 1 hPa, 9908 (No GWD)
275.0
270.0
265.0
260.0
255.0
250.0
50
0
-50
Latitude
0
100
200
300
Longitude

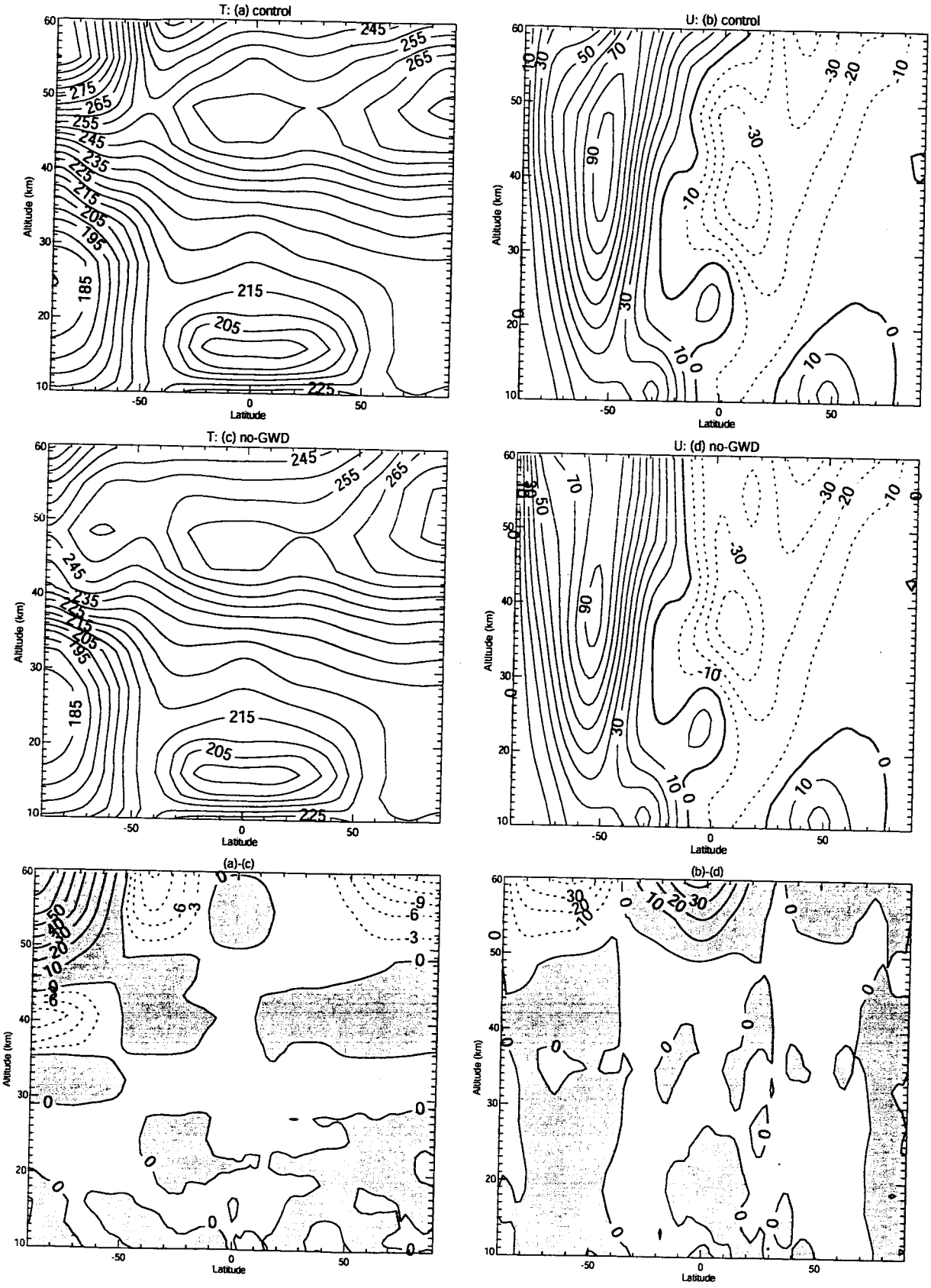
T: (a) control
U: (b) control
T: (c) no-GWD
U: (d) no-GWD
(a)-(c)
(b)-(d)
Altitude (km)
Latitude

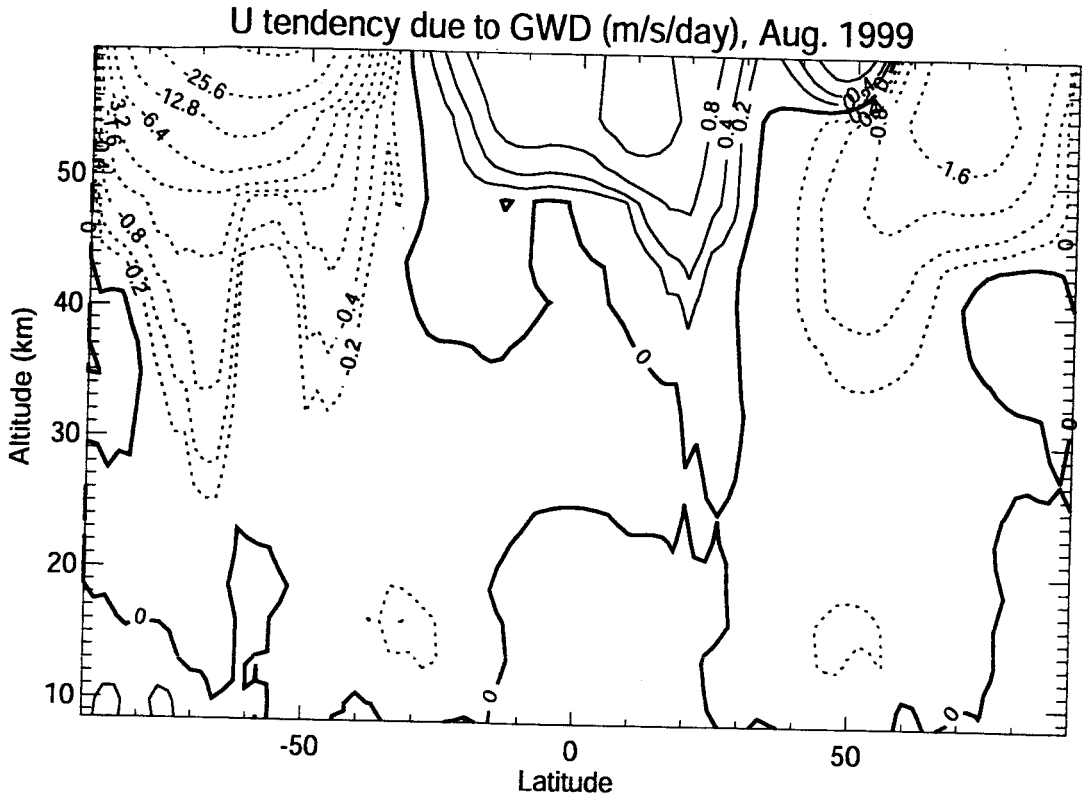
U tendency due to GWD (m/s/day), Aug. 1999
Altitude (km)
Latitude
50
40
30
20
10
-50
0
50
-25.6
-12.8
-6.4
-3.2
-1.6
-0.8
-0.4
-0.2
0
0.2
0.4
0.8

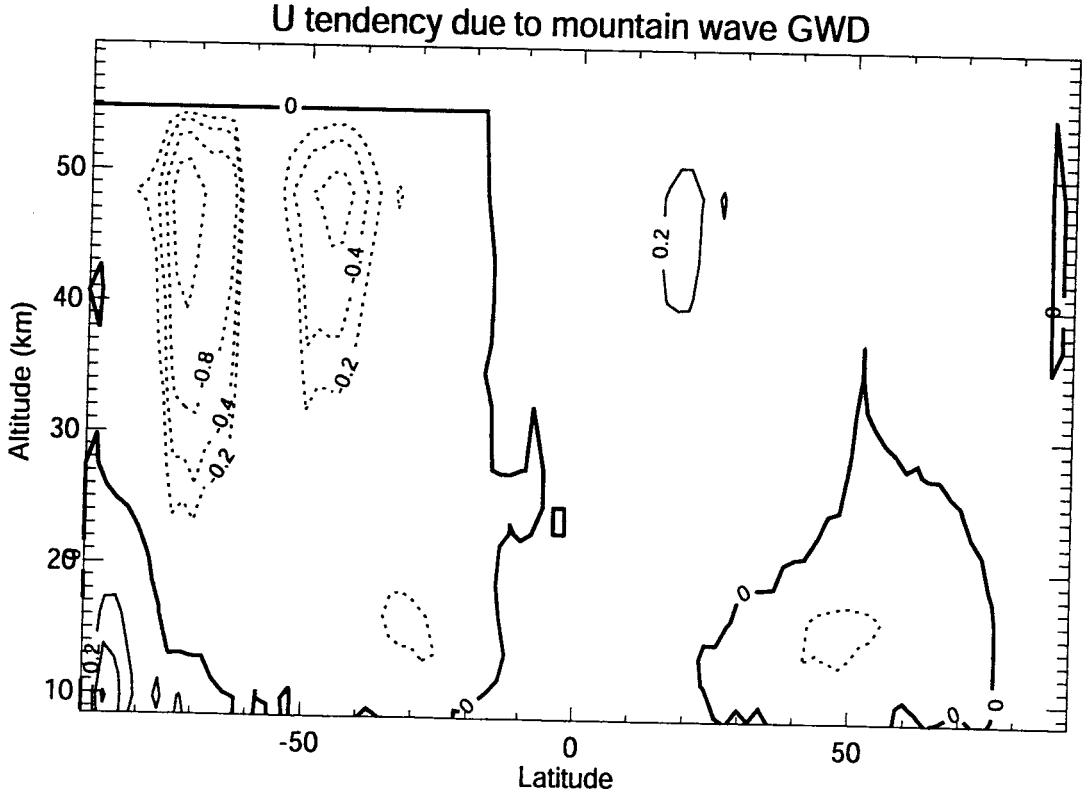
U tendency due to mountain wave GWD
Altitude (km)
Latitude
50
40
30
20
10
-50
0
50
-0.8
-0.4
-0.2
0
0.2

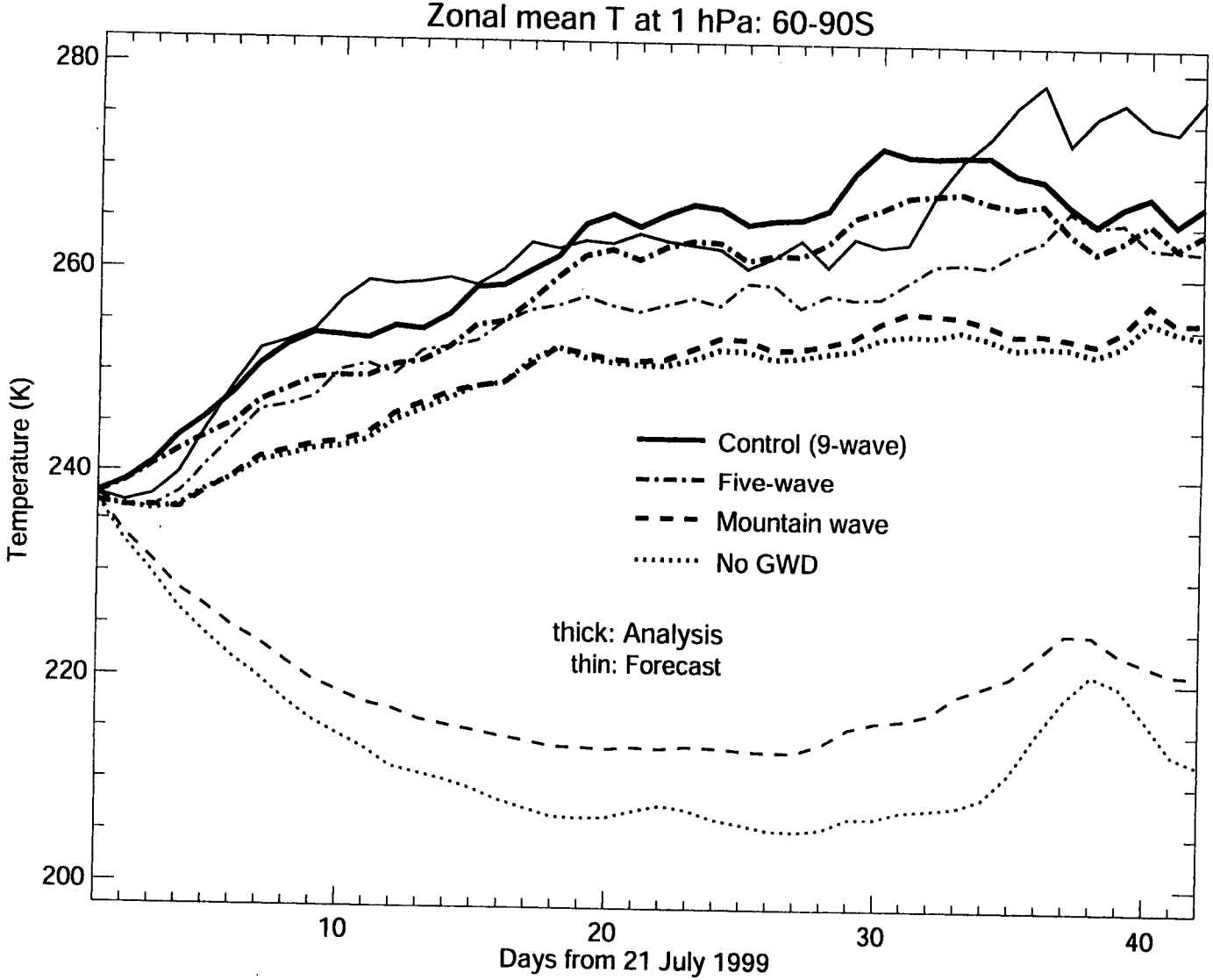
Zonal mean T at 1 hPa: 60-90S
Temperature (K)
280
260
240
220
200
10
20
30
40
Days from 21 July 1999
Control (9-wave)
Five-wave
Mountain wave
No GWD
thick: Analysis
thin: Forecast

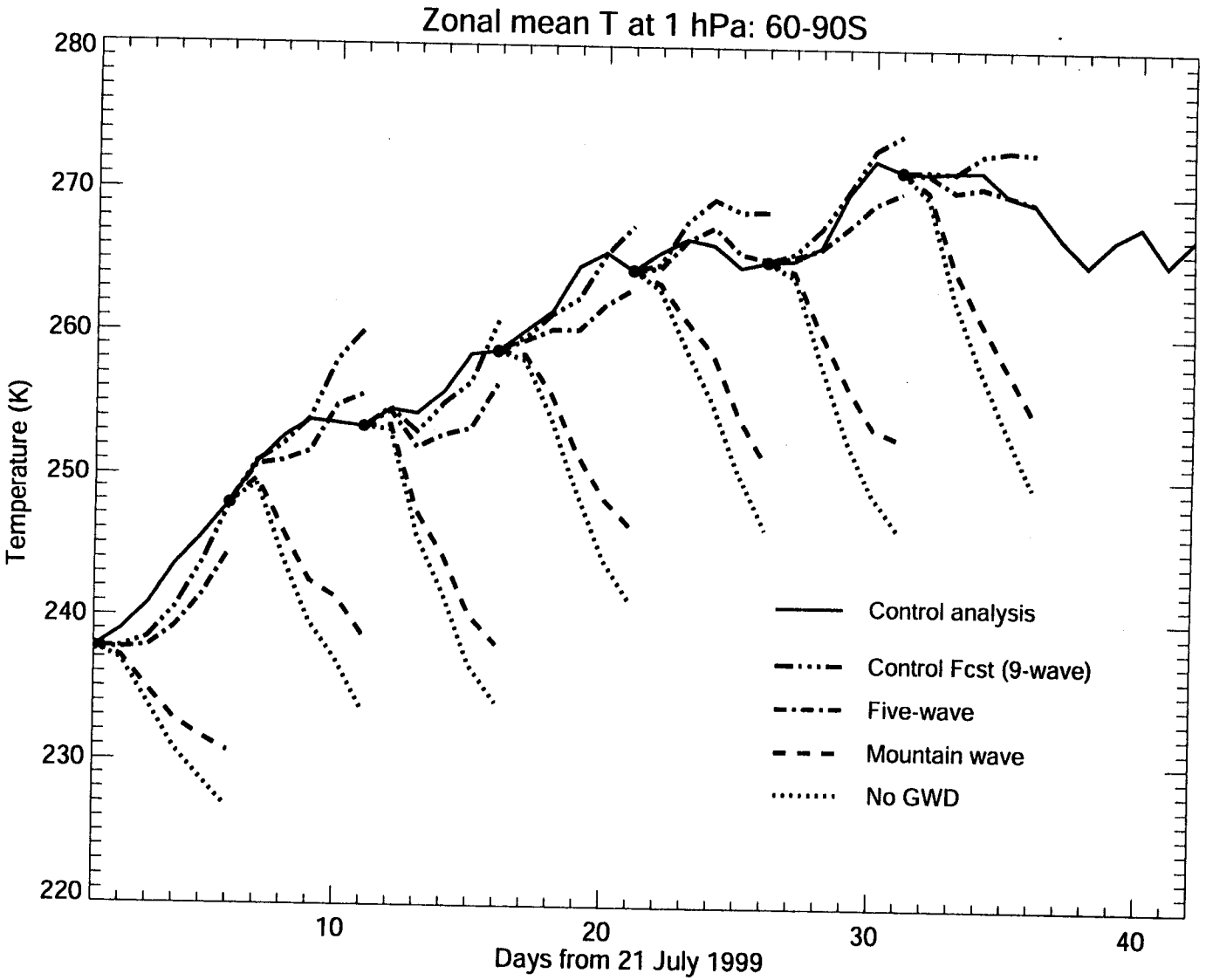
Zonal mean T at 1 hPa: 60-90S
Temperature (K)
280
270
260
250
240
230
220
10
20
30
40
Days from 21 July 1999
Control analysis
Control Fcst (9-wave)
Five-wave
Mountain wave
No GWD

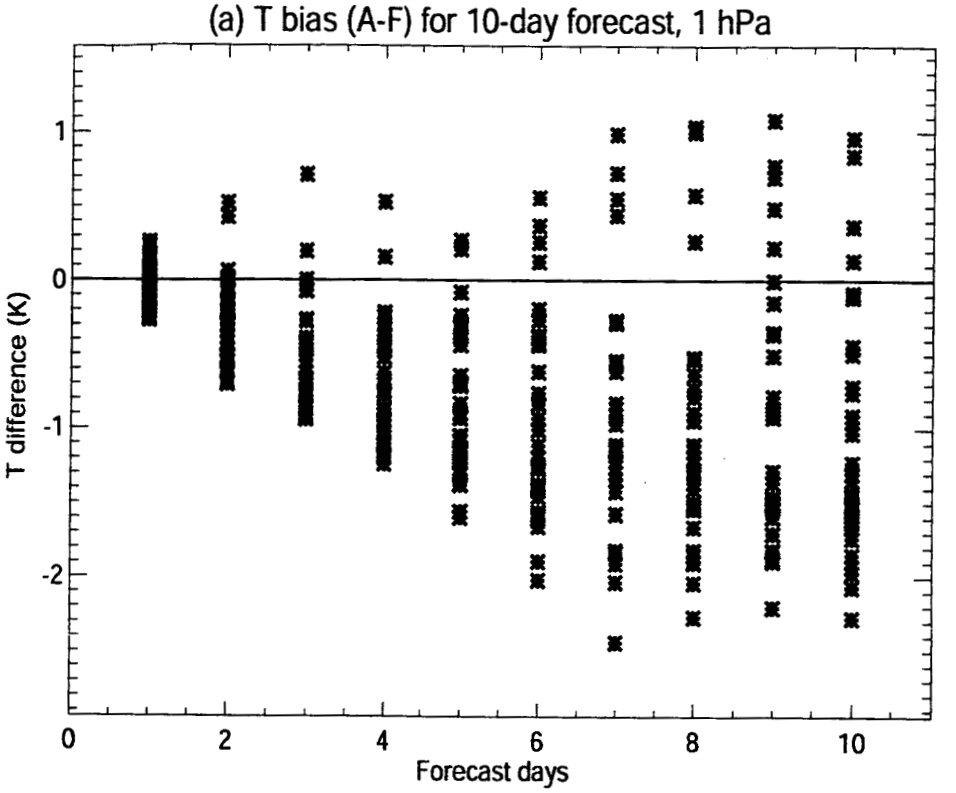
(a) T bias (A-F) for 10-day forecast, 1 hPa
T difference (K)
1
0
-1
-2
0
2
4
6
8
10
Forecast days

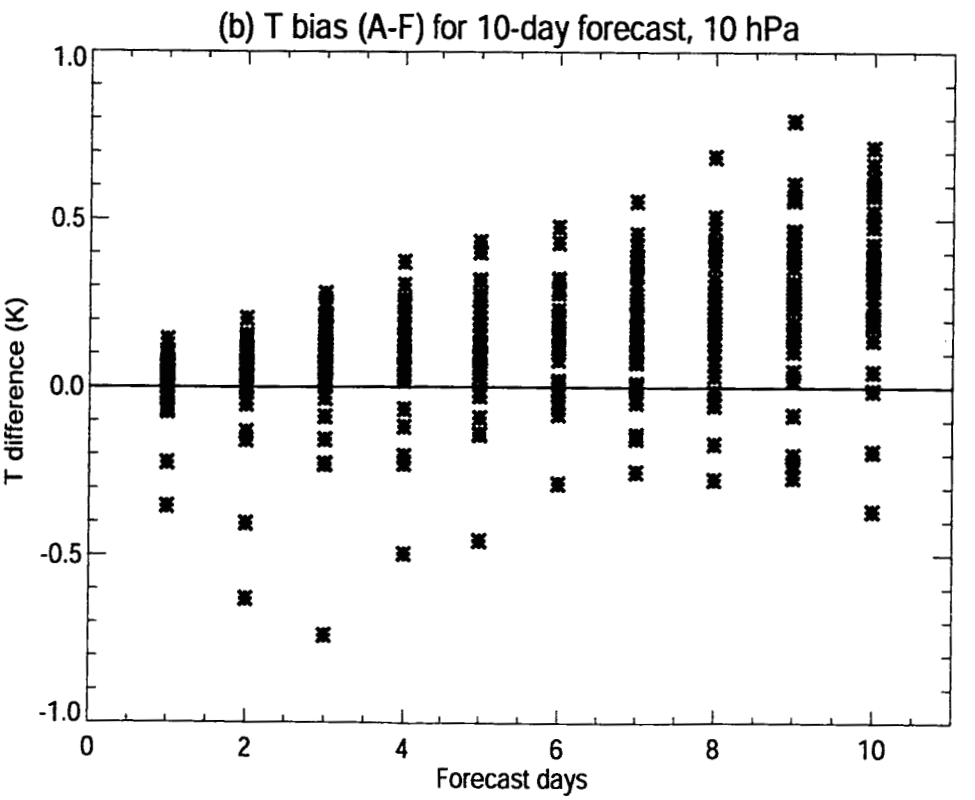
(b) T bias (A-F) for 10-day forecast, 10 hPa
T difference (K)
1.0
0.5
0.0
-0.5
-1.0
0
2
4
6
8
10
Forecast days

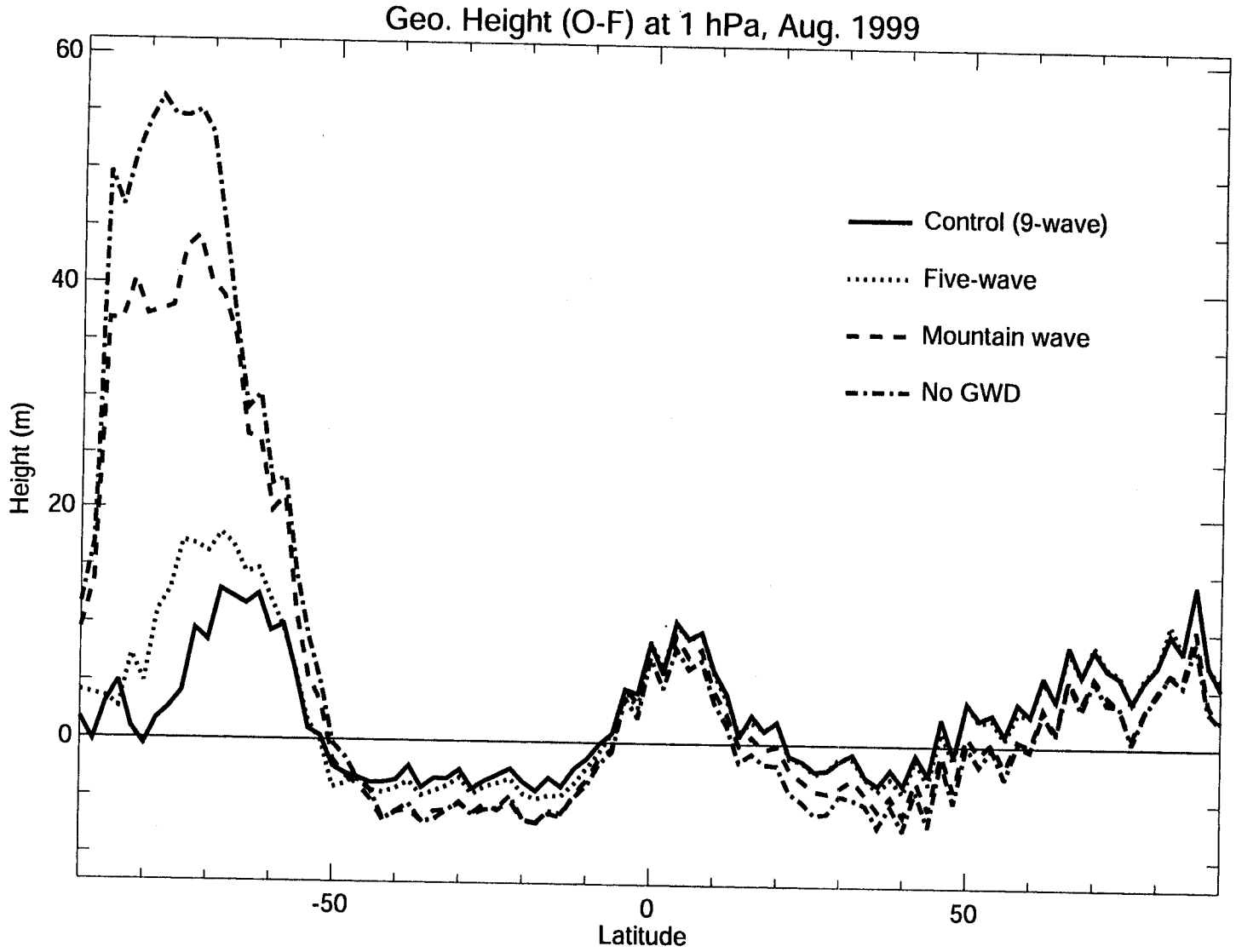
Geo. Height (O-F) at 1 hPa, Aug. 1999
60
40
20
0
Height (m)
-50
0
50
Latitude
Control (9-wave)
Five-wave
Mountain wave
No GWD

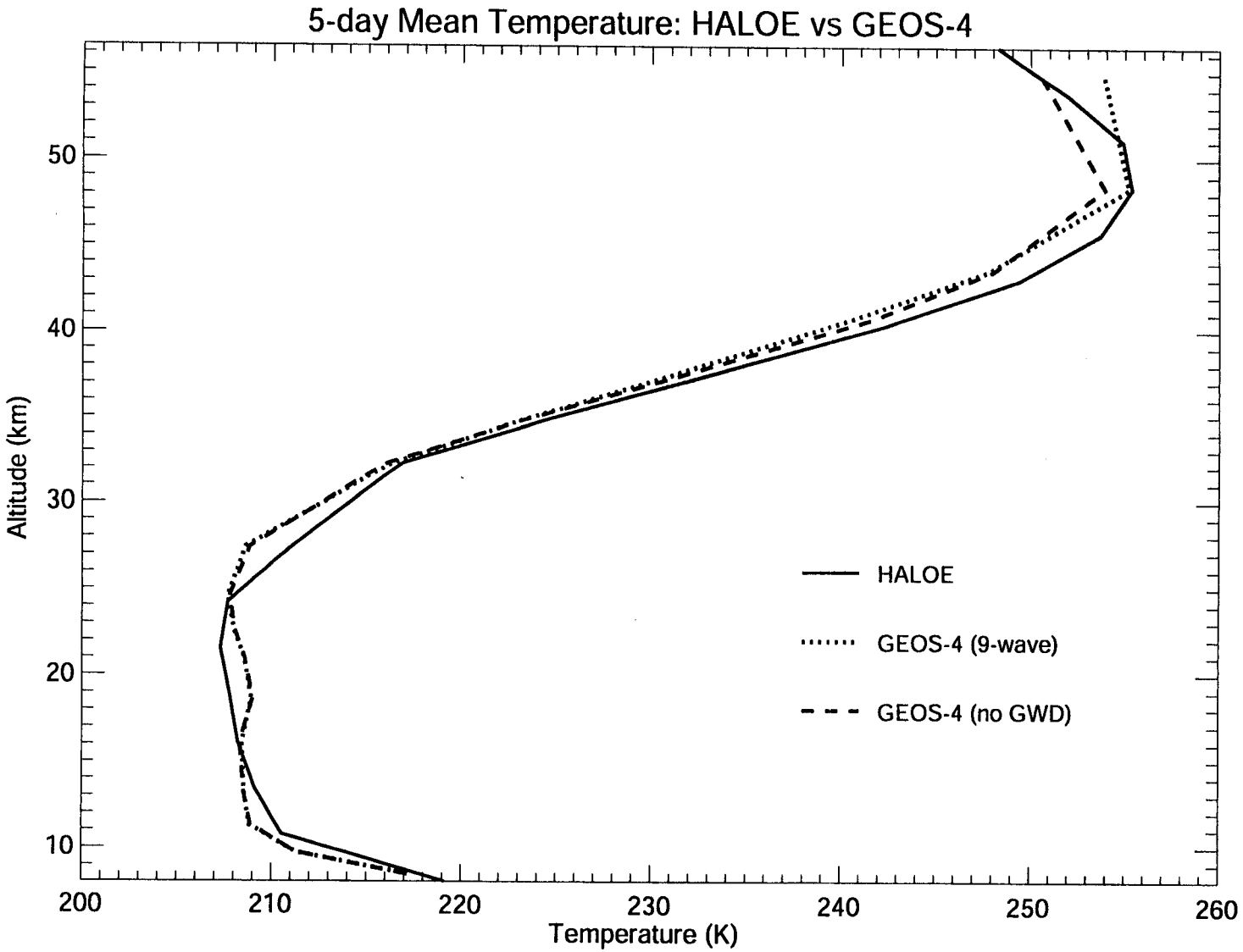
5-day Mean Temperature: HALOE vs GEOS-4
Altitude (km)
50
40
30
20
10
200
210
220
230
240
250
260
Temperature (K)
HALOE
GEOS-4 (9-wave)
GEOS-4 (no GWD)